Published in final edited form as:
Arterioscler Thromb Vasc Biol. 2014 July ; 34(7): 1399–1411. doi:10.1161/ATVBAHA.114.303508.

S100/calgranulin-mediated inflammation accelerates left ventricular hypertrophy and aortic valve sclerosis in chronic kidney disease in a RAGE dependent manner

Ling Yan, M.D., Ph.D.,
Department of Medicine, Cardiology, The University of Chicago, IL 60637

Liby Mathew, MS,
Department of Medicine, Nephrology, The University of Chicago, IL 60637

Bijoy Chellan, Ph.D.,
Department of Medicine, Cardiology, The University of Chicago, IL 60637

Brandon Gardner, MS,
Department of Medicine, Cardiology, The University of Chicago, IL 60637

Judy Earley,
Department of Medicine, Cardiology, The University of Chicago, IL 60637

Tipu S. Puri, M.D., and
Department of Medicine, Nephrology, The University of Chicago, IL 60637

Marion A. Hofmann Bowman, M.D., Ph.D.*
Department of Medicine, Cardiology, The University of Chicago, IL 60637

Abstract

Objective—S100A12 and fibroblast growth factor 23 (FGF23) are biomarkers of cardiovascular morbidity and mortality in patients with chronic kidney disease (CKD). We tested the hypothesis that human S100/calgranulin would accelerate cardiovascular disease in mice subjected to CKD.

Approach and Results—A bacterial artificial chromosome of the human S100/calgranulin gene cluster containing the genes and regulatory elements for S100A8, S100A9 and S100A12 was expressed in C57BL/6J mouse (hBAC-S100) to generate a novel humanized mouse model. CKD was induced by ureteral ligation and hBAC-S100 mice and WT mice were studied after 10 weeks of chronic uremia. hBAC-S100 mice with CKD showed increased FGF 23 in the hearts, left ventricular hypertrophy (LVH), diastolic dysfunction, focal cartilaginous metaplasia and calcification of the mitral and aortic valve annulus together with aortic valve sclerosis. This phenotype was not observed in WT mice with CKD or in hBAC-S100 mice lacking the receptor for advanced glycation endproducts (RAGE) with CKD, suggesting that the inflammatory milieu mediated by S100/RAGE promotes pathological cardiac hypertrophy in CKD. In vitro,

*To whom correspondence should be addressed: Marion A. Hofmann Bowman, The University of Chicago, 5841 S. Maryland Avenue MC 6088, Chicago, IL 60637, T: 773 834 0807 F: 773 702 2681, mhofmann@medicine.bsd.uchicago.edu.

Disclosure: All authors declare no conflict of interest.

inflammatory stimuli including IL-6, TNFα, LPS, or serum from hBAC-S100 mice up regulated FGF23 mRNA and protein in primary murine neonatal and adult cardiac fibroblasts.

Conclusions—Myeloid-derived human S100/calgranulin is associated with the development of cardiac hypertrophy and ectopic cardiac calcification in a RAGE dependent manner in a mouse model of CKD. We speculate that FGF23 produced by cardiac fibroblasts in response to cytokines may act in a paracrine manner to accelerate LVH and diastolic dysfunction in hBAC-S100 mice with CKD.

Keywords

S100 proteins; RAGE; chronic kidney disease; LVH; ectopic cardiac calcification

Chronic kidney disease (CKD) is a global health problem and is associated with accelerated cardiovascular disease, the leading cause of premature death among patients with CKD [1]. Several factors contribute to cardiovascular morbidity in CKD including oxidative stress, inflammation, dyslipidemia, hypertension, atherosclerosis, vascular calcification, and left ventricular dysfunction among others. Epidemiological studies in dialysis patients have identified serum S100A12 levels as a significant and independent determinant for carotid intimal media thickness [2, 3], peripheral artery disease [4] and as a predictor for cardiovascular mortality [5–7]. The origin of the elevated S100A12 serum levels in patients with CKD and other chronic or acute inflammatory disease is not clear, but leucocytes are a possible source since these cells are the major producer of S100A12, and the molecule is released from dying leucocytes or upon activation. This is supported by recent findings by Hara et al., demonstrating a strong correlation between S100A12 mRNA in leucocytes and serum S100A12 concentrations in uremic CKD patients[8]. S100/calgranulin binds to and activates the receptor for advanced glycation end products, RAGE, and thereby promotes vascular inflammation [9–11]. This suggests that S100A12 could directly participate in cardiovascular disease, rather than just serve as a biomarker of inflammation.

S100A12 and homolog S100A8/9 (also known as S100/calgranulins) belong to the family of EF-hand calcium binding proteins and are endogenously expressed in myeloid cells, particularly in neutrophil granulocytes where they comprise 5% and 40% of cytosolic proteins, respectively [12, 13]. Accordingly, elevated serum concentrations of S100/calgranulins are associated with acute and chronic inflammatory diseases. In addition to their endogenous expression in myeloid cells, S100/calgranulins are induced in human vascular smooth muscle under pathological conditions, such as atherosclerosis [14], coronary artery plaque rupture [15], ischemia [16], aortic aneurysms and dissections [17], and in murine smooth muscle in response to endothelial injury [18]. Recently, our laboratory demonstrated in mice engineered to express human S100A12 driven by the smooth muscle 22-α promoter, osteochondrocytic reprogramming of vascular smooth muscle cells (VSMC) with activation of osteoblastic genes leading to accelerated atherosclerosis and vascular calcification when exposed to hyperlipidemia [19], or when exposed to surgically induced CKD [20].

The present study was designed to test the hypothesis that elevated levels of S100/calgranulin in myeloid cells and serum in mice with CKD would accelerate pathological cardiac remodeling and to identify potential underlying mechanisms. To test this hypothesis,

we exploited the fact that S100A12 is not present in mice[21] and generated transgenic mice expressing human S100/calgranulin proteins in cells and tissues similar to the expression pattern in humans, by utilizing a bacterial artificial chromosome containing 60 kbp of human DNA of the S100 gene cluster containing the genes and regulatory DNA for S100A8, S100A12, and S100A9 (hBAC-S100 mice). hBAC-S100 and wild type (WT) littermate mice were subjected to a protocol of renal injury and their hearts were studied 10 weeks after exposure to elevated blood urea nitrogen (BUN). We found cardiac hypertrophy and diastolic dysfunction together with focal cartilaginous metaplasia and calcification in the fibroblast-rich annulus of the mitral and aortic valves, thickening of the aortic valve leaflets in hBAC-S100 mice with CKD, but not in WT mice with CKD. We identified S100/calgranulin-mediated inflammation, at least in part, as an underlying mechanism of this pathological cardiac remodeling, since hBAC-S100 mice lacking RAGE had attenuated systemic inflammation and did not develop pathological cardiac remodeling when exposed to the same degree of CKD.

Our data presented here implicate S100/RAGE for the first time that as an accelerating factor for the development of cardiac hypertrophy and diastolic dysfunction in CKD. Our data suggest that enhanced fibroblast growth factor 23 (FGF23) secretion in cardiac fibrous tissue may promote processes leading to cardiac hypertrophy and diastolic dysfunction.

Material and Methods

Materials and Methods are available in the online-only Data Supplement.

Results

1. Enhanced inflammation in hBAC-S100 mice

Transgenic mice were generated by utilizing a bacterial artificial chromosome containing 60 k bp of human DNA of the S100 gene cluster containing only the genes for human S100A8, S100A9 and S100A12 and regulatory DNA. We found transgenic expression of human S100A12 protein in myeloid blood cells (Figure 1A) and in the serum of hBAC-S100 mice (Figure 1B). S100A12 is co-expressed in myeloid cells with endogenous murine S100A8, and as expected, S100A12 protein was not detected in myeloid cells and in the serum of WT mice [21]. Interestingly, despite expression on hS100A8/9 mRNA in peripheral blood leucocytes, serum concentration of S100A8/9 was similar in both groups, even when measured using antibodies that recognize both murine and human S100A8/9. S100A12 mRNA was detected at high levels in white blood cells (WBC), bone marrow, spleen, and at much lower expression levels in all other organs tested including heart, aorta, kidney, skin, lung, and muscle. S100A12mRNA was not detected in cultured cardiac fibroblasts and cardiomyocytes harvested from hBAC-S100 hearts, and at very low level in whole heart tissue when normalized to the abundant expression of myosin heavy chain 7 (0.00066 and 1, respectively) (Figure 1C). Clinically, transgenic mice appear and develop normally and are fertile. There was no difference in the counts for leucocytes, segmented neutrophils, lymphocytes, platelets and hemoglobin, as well as serum AST, ALT, creatinine, and total serum cholesterol (data not shown). Differential gene expression in WBC from 6-week old animals was first tested by microarray (IlluminaWG-6v2, Supplement Table 1A–C), and

selected genes were verified by qRT-PCR. As shown in Figure 1D, we found a 3–45 fold increase in gene expression associated with inflammation or neutrophil activation including LPS-binding protein, myeloperoxidase, neutrophil lactoferrin, vascular cell adhesion molecule 1, neutrophil proteinase 4, CD177, neutrophil gelatinase associated lipocalin, bone marrow proteoglycan 2, CCAAT/enhancer binding protein epsilon, cathepsin G and chitinase 3-like 3, which was attenuated in hBAC-S100 mice lacking RAGE (Figure 1E). Consistent with prior findings [9, 22, 23], overexpression of S100/calgranulin led to a sustained inflammatory milieu with increased IL-6 and IL-22 (Figure 1F,G), which was abolished in hBAC-S100 mice lacking RAGE (Figure 1H).

2. Model of surgically induced chronic kidney disease

10-weeks old hBAC-S100 mice and WT littermate mice were subjected to reversible right ureteral obstruction (RUO) for 6 days, followed by irreversible left ureteral obstruction (LUO) to induce a moderate degree of chronic kidney disease (Figure 2A)[20]. Sham-operated mice underwent repeated anesthesia and laparotomy with inspection of the ureter. Serum BUN was elevated approximately 2.5-fold in mice after LUO compared to sham-operated mice ($P<0.0001$), and there was no significant difference in BUN among different groups of mice undergoing ureteral obstruction (Figure 2B). In parallel, serum creatinine was significantly elevated in all mice with CKD compared to sham (0.37±0.12 vs. 0.14±0.09 mg/dl, $P<0.001$). Moreover, calcium and phosphorus were not different between hBAC-S100 and WT mice undergoing ureteral ligation, indicating that S100/calgranulin had no direct effect on the severity of CKD, or degree of hyperphosphatemia in this model. Furthermore, there were no differences in the degree of tubular atrophy, interstitial fibrosis and interstitial inflammation upon light microscopy of the right kidney, indicating that transgenic expression of S100/calgranulin had no major effect on the response to reversible right ureteral ligation injury (Figure 2C and 2D). The repeated surgeries were well tolerated, and there were no significant differences in body weight across the four groups of mice (data not shown). As previously reported in other mouse models of hydronephrosis [24], systolic and diastolic blood pressure leves were significantly elevated in mice with CKD compared to sham-operated mice, although there was no significant difference between hBAC-S100 and WT mice within their respective groups (Figure 2E). Similar to previous findings of elevated serum FGF23 after 5/6 nephrectomy [25], we found significantly elevated FGF23 in the serum of mice after ureter ligation. FGF23 was similar between sham-operated WT and hBAC-S100 mice, and significantly increased in mice with CKD without any significant difference between hBAC-S100 and WT-CKD mice within their respective groups (Figure 2F). This suggests that S100/calgranulin, at least in this animal model of CKD, does not independently contribute to elevated serum FGF23. In contrast, serum hS100A12 increased further in hBAC-S100 mice with CKD when compared to sham-operated hBAC-S100 mice (42±17 ng/ml and 25±7 ng/ml, $P=0.04$, Figure 2G), suggesting that the metabolic changes associated with CKD promote the release of S100A12 from myeloid cells. Moreover, the serum concentration of S100A12 in hBAC-S100 mice was comparable to concentration measured simultaneously in 10 human serum samples (mean 28.2 ±29 ng/ml), indicating that this novel transgenic hBAC-S100 mouse model is compatible to human physiology with regards to S100A12 expression.

3. S100/calgranulin accelerates left ventricular hypertrophy and diastolic dysfunction in CKD

In order to determine whether mice with increased serum concentration of S100/calgranulin would be more susceptible to pathological cardiac remodeling, we performed detailed in vivo cardiac echocardiography. As shown in Figure 3, systolic left ventricular function measured by fractional shortening (FS) was similar in all four groups (Figure 3A, and quantified in D). Left ventricular posterior wall thickness was similar between sham-operated mice, but was significantly increased in hBAC-S100 mice with CKD compared to WT-CKD mice (Figure 3A, and quantified in E). Diastolic function measured by the ratio of Early to Atrial (E/A) mitral flow was similar between sham-operated mice, but significantly reduced in hBAC-S100 mice with CKD compared to WT-CKD mice (Figure 3B and quantified in F). This suggests that hBAC-S100 mice challenged with CKD are more prone to develop left ventricular hypertrophy and abnormal diastolic function. Consistent with this finding, peak aortic valve velocity time integral (AoVTI) was significantly increased in hBAC-S100 with CKD compared to WT-CKD mice, while it was similar between sham-operated mice (Figure 3C and quantified in G). In contrast, mean AoVTI was similar between all four groups, suggesting that the accelerated peak aortic flow possibly stems from increased LV force and/or mild aortic valve abnormalities but without obstructive aortic valve stenosis hBAC-S100 with CKD. Left ventricular hypertrophy (LVH) in hBAC-S100/CKD mice was confirmed upon necropsy and representative cardiac sections of the mid-cavity are shown in Figure 3H. The absolute heart weight was significantly increased in hBAC-S100/CKD compared to WT/CKD (188±26 mg and 141±19 mg; respectively, $P<0.04$), and was also increased when indexed to body weight (Figure 3I). In contrast, sham operated WT and hBAC-S100 mice had equal left ventricular posterior wall thickness (Figure 3E), and similar heart weights (138 ± 17 mg and 136 ±15 mg; respectively). This indicates that transgenic expression of S100/calgranulin in the absence of CKD is not sufficient to induce cardiac hypertrophy in mice aged up to 5-months.

Taken together, our data indicate that expression of human S100/calgranulin in mice challenged with CKD promotes LVH, abnormal diastolic function and mildly accelerated peak flow across the aortic valve.

4. LVH and diastolic dysfunction in hBAC-S100/CKD mice is associated with aortic valve sclerosis and ectopic cardiac calcification

Next we examined serial cardiac sections stained for H&E, Masson's Trichrome, Verhoeff van Giessen and Alizarin Red systematically from the apex through the ascending aorta. Hypertrophic cartilage cells and calcification foci were present in all hearts from hBAC-S100 mice with CKD, while this was almost completely absent in WT-CKD hearts (Figure 4). The chondrocytic hypertrophy and calcification were most often located in the fibrous tissue of the mitral valve annulus and aortic valve annulus, and there was very scant calcification of cardiomyocytes in the left or right ventricle. A representative histology of chondrocytic hypertrophy with calcification in the mitral valve annulus is shown in Figure 4A, and of the aortic valve annulus in Figure 4B. Consistent with increased peak AoVTI on echocardiography, hBAC-S100 with CKD showed significantly thicker aortic valve leaflets but without overt calcification (Figure 4B and E). Abnormal aortic valve thickness,

chondrocytic hypertrophy and calcification were absent in all age-matched hBAC-S100 and WT mice undergoing sham surgery, indicating that the metabolic milieu of CKD accelerates valvular pathology in S100/calgranulin transgenic mice. However, hBAC-S100 mice aged to 10–12 months also developed enhanced calcification visualized by Alizarin Red staining which was near absent in age-matched WT littermate mice (Figure 4C), indicating that the expression of hS100/calgranulin is sufficient to mediate hypertrophic cartilage cells and cardiac calcification even in the absence of CKD. Calcification was located in the aged hBAC-S100 mice mostly near the aortic valve annulus and occasionally on the AV leaflet tip (and very infrequently at the mitral valve annulus), and a representative histology of a 10 month- old animal is shown in Figure 4C. AV thickness did not differ between 10–12 month-old hBAC-S100 and WT littermate mice, with both groups of aged mice having significantly thicker valves compared to their respective group of younger mice (Figure 4E).

5. hBAC-S100 mice with CKD have increased cardiac expression of FGF23 and left ventricular hypertrophy

Due to the increased left ventricular posterior wall thickness upon in vivo echocardiography and confirmed left ventricular hypertrophy upon necropsy in hBAC-S100 mice with CKD, we probed cardiac tissue for mRNA expression linked to cardiac hypertrophy and fibrosis. As expected, the expression of genes characteristic of LVH including β-MHC, ANP and TGF-β and others were increased in hBAC-S100 hearts. Notably, FGF23 mRNA was 6.8-fold increased in hBAC-S100 mice with CKD compared to WT-CKD ($P<0.001$, Figure 5A). Interestingly serum concentration of FGF23 has recently emerged in several epidemiological studies as a biomarker predicting cardiovascular complications in patients with CKD, and a dose-dependent association between elevated FGF23 levels and a greater risk of major cardiovascular events and mortality has been demonstrated [26, 27]. A plausible explanation linking high FGF 23 to greater cardiovascular risk was offered by studies in which elevated FGF23 was independently associated with left ventricular hypertrophy, and FGF23 was recently shown to directly induce cardiac hypertrophy in a paracrine manner [25].

Importantly, FGF23 protein was increased by 2.6- fold in the cardiac tissue lysates harvested from hBAC-S100/CKD mice (Figure 5B). FGF23 mRNA and protein was expressed at very low levels in the heart of sham mice, and there was no significant difference between sham-operated WT and hBAC-S100 mice (data not shown).

Immunohistochemistry of serial cardiac sections demonstrated that FGF23 was expressed in valvular interstitial cells of hBAC-S100/CKD hearts (Figure 5D), and only minimally in cardiac fibrous tissue from WT/CKD (Figure 5G). Neonatal bone control tissue was used as positive control tissue (Figure 5I). The mRNA levels for cardiac expression of potential receptors for FGF23, namely FGFR1, FGFR2, FGFR3, FGFR4, and Klotho were not different between hBAC-S100/CKD and WT/CKD (data not shown).

Since mineralizing cells such as osteoblasts and chondroblasts are a principal source of FGF23 [28], we probed whether cardiac cells exposed to a milieu conducive to the promotion of chondroplastic metaplasia and enhanced mineralization would up-regulate FGF23 in cardiac cells. As shown in Supplement Figure 1, neonatal cardiac fibroblasts from WT hearts did not increase FGF23 mRNA in response to high-phosphate medium supplemented

either with rS100A12 (1ug/ml) or control BSA cultured for up to 20 days. As expected, genes important for the regulation of mineralization including osteocalcin (BGLAP), osteopontin (OPN) and Matrix gla protein (MGP), previously found at increased levels in calcific aortic valves of uremic animal models[29, 30], increased in response to high-phosphate calcification medium. While rS100A12 did not alter expression of FGF23, rS100A12 reduced significantly gene expression of osteopontin by 20% to 40% (Supplement Figure 1C). This suggests that S100/calgranulin may influence osteopontin regulation in cardiac fibroblasts, but may not directly promote expression of FGF 23 in cardiac fibroblasts. We therefore hypothesized that systemic intermediary products in vivo might affect FGF23 expression in cardiac fibroblasts in hBAC-S100 mice subjected to CKD. We next studied whether cytokines might promote FGF23 expression in cardiac fibroblasts. As shown in Figure 5K, we found a robust and significant increase in FGF23 mRNA levels in response to cytokines in cardiac fibroblast and aortic smooth muscle cells when stimulated with low dose cytokines including IL-6 (25 ng/ml), TNFα (25 ng/ml) and LPS (25 ng/ml). In contrast, recombinant S100A12 (up to 2μg/ml) did not induce FGF23. However, stimulation with serum from hBAC-S100 mice up regulated FGF23 mRNA 2–3 fold compared to WT serum. Moreover, FGF23 protein was significantly elevated in the cell culture supernatant harvested from cardiac fibroblasts stimulated with either cytokines or serum from hBAC-S100 mice. Interestingly, cardiac fibroblasts lacking RAGE had the same robust up regulation of FGF23 protein in response to cytokines than cardiac fibroblasts with intact RAGE signaling (Figure 5L).

Taken together, our study shows that S100/calgranulin is sufficient to enhance pathological cardiac remodeling in mice with CKD with several pathological findings including LVH and impaired diastolic function, hypertrophic cartilage cells in the aortic and mitral valve annulus with spotty calcification in the valve annulus, increased aortic valve thickening with mild AV dysfunction, and increased cardiac expression of FGF23, likely in response to the enhanced inflammation present in hBAC-S100 mice.

6. Pathological cardiac remodeling in hBAC-S100 mice with CKD is dependent on receptor for advanced glycation endproducts (RAGE)

To gain more insight into underlying molecular signaling cascades of S100/calgranulins resulting in pathological cardiac remodeling, we utilized mice lacking RAGE and tested whether RAGE is required to mediate these effects. hBAC-S100 mice were bred with homozygote RAGE knockout mice [31], and hBAC-S100/RAGE$^{-/-}$ and the WT/RAGE$^{-/-}$ littermate mice were subjected to the same protocol of surgically induced-CKD. As shown in Figure 2B, BUN increased equally in hBAC-S100/RAGE$^{-/-}$ and WT/RAGE$^{-/-}$ mice subjected to CKD by approximately 2.5 fold, and this was similar to the BUN levels achieved in mice with intact RAGE signaling. Moreover, serum creatinine (0.34 ±0.13 mg/dl and 0.37 ±0.17, P=NS), serum phosphate (7.46 ±0.83 and 7.3 ±0.83, P=NS), and S100A12 (34± 14 and 42±17 ng/ml, P=0.09) were similar between hBAC-S100/RAGE$^{-/-}$ with CKD and hBAC-S100/RAGE$^{+/+}$ with CKD. There was no difference in the semi-quantitative scoring of kidney pathology upon light microscopy between all the groups of mice with reversible ureteral ligation (Figure 2C and D). Moreover, systolic, diastolic and mean blood pressure levels were similar between in RAGE null mice with and without

transgenic expression of human S100/calgranulin (Figure 6A), and the blood pressure levels were not different from CKD mice with intact RAGE signaling. Serum FGF23 was similar between the WT/RAGE$^{-/-}$/CKD and hBAC-S100/RAGE$^{-/-}$/CKD (425±31 pg/ml and 526±28 pg/ml), but was significantly reduced in the WT/RAGE$^{-/-}$/CKD mice compared to WT/RAGE$^{+/+}$/CKD mice (425±31 and 630±48, respectively, P=0.03, Figure 6B). In parallel with reduced IL-6 and IL-22 in hBAC-S100 mice lacking RAGE as shown in Figure 1H, hBAC-S100/RAGE$^{-/-}$ mice were protected from developing cardiac hypertrophy. The absolute heart weight (137±22 mg and 134±19 mg; respectively, P=NS) or indexed heart weight was similar between WT/RAGE $^{-/-}$ and hBAC-S100/RAGE$^{-/-}$ (Figure 6C). Moreover, there was no difference between hBAC-S100/RAGE$^{-/-}$ and WT/RAGE$^{-/-}$ littermates in the gene expression of genes linked to hypertrophy and fibrosis, including FGF23, βMHC, ANP, TGFβ, Smad2, CTGF and Col1a1(Figure 6D). This was further confirmed by immunoblotting in cardiac tissue lysates, and FGF23 protein was equally low in WT/RAGE$^{-/-}$ and in hBAC-S100/RAGE $^{-/-}$ mice with CKD, in contrast to the increased FGF23 protein in cardiac lysates from hBAC-S100 mice with intact RAGE signaling (Figure 6E and quantified in F). Lastly, cardiac echocardiography in hBAC-S100/RAGE$^{-/-}$/CKD and WT/RAGE$^{-/-}$/CKD demonstrated normal left ventricular systolic function (FS 46±7% and 42±8%, P=NS), preserved diastolic function measured by continuous Doppler inflow over the mitral valve (Figure 6G), normal mean and peak AoVTI (989 ±54 mm/s and 1021 ±47 mm/s, P=NS and 1589 ±97 and 1498 ±102 mm/s, P=NS; respectively). Left ventricular posterior wall thickness on M-mode echocardiography was similar in hBAC-S100/RAGE$^{-/-}$/CKD (0.51 ±0.08 mm), WT/RAGE$^{-/-}$/CKD (0.57 ±0.09 mm), and control WT/RAGE$^{+/+}$-sham mice (0.59 ±0.06 mm).

Together with normalization of inflammation and pathological cardiac hypertrophy in hBAC-S100/RAGE$^{-/-}$, we found no significant focal cartilaginous metaplasia or cardiac calcification in mice lacking RAGE, and the scant calcification seen in the hBAC-S100/RAGE$^{-/-}$ mice was similar to WT mice (Figure 6H). This was accompanied by normal thickness of the aortic valve leaflets and there was no difference between hBAC-S100/RAGE$^{-/-}$ mice with CKD, WT/RAGE$^{-/-}$ with CKD, and WT/RAGE^{+}/$^{+}$ mice with CKD (61μm ±7, 59 μm ±4 and 62 μm ±8, respectively).

Taken together, our data demonstrate that S100/calgranulin promotes maladaptive cardiac remodeling in a RAGE-dependent manner in metabolically-challenged mice that mimic conditions of human chronic kidney disease, i.e. increased serum concentration of BUN and S100/calgranulin. S100/calgranulin promotes systemic inflammation and our invitro data suggest that up regulation of FGF23 in cardiac fibroblast's in response to cytokines might be a potential link between systemic inflammation and development of cardiac hypertrophy and diastolic dysfunction in vivo.

Discussion

Left ventricular hypertrophy and diastolic dysfunction as well as vascular and cardiac calcification are commonly associated with chronic kidney disease and contribute to the high incidence of heart failure and cardiovascular mortality observed among patients with CKD and end stage renal failure. While cardiac remodeling comprises a multifactorial and

complex network in response to the metabolic and hemodynamic abnormalities associated with CKD, both serum S100A12 [5–7], and serum FGF23 [25, 26, 32, 33] have been identified as powerful predictors of cardiovascular mortality in end stage renal disease, suggesting a possible synergistic mechanism between S100A12 and FGF23. Our study, utilizing a novel "humanized" mouse model with transgenic expression of hS100/calgranulin in myeloid cells and increased levels of circulating S100/calgranulin protein, demonstrates that S100/calgranulin is sufficient to promote left ventricular hypertrophy and ectopic cardiac calcification in animals with chronic kidney disease, and this process is dependent on RAGE, a pattern recognition receptor for multiple ligands including S100/calgranulins. Although hS100A8/9 mRNA was detected in myeloid cells, bone marrow and spleen in hBAC-S100 mice, the serum concentration of S100A8/9, which likely is a composite of human and murine S100A8/9, was not increased compared to WT serum. We suspect that release of S100A8/9 from hematopoietic cells is regulated beyond mRNA levels.

In vivo, we demonstrate that transgenic expression of S100/calgranulin leads to augmented expression of FGF23 in interstitial fibroblasts and the appearance of hypertrophic cartilage cells in the aortic and mitral valve annulus. It is tempting to speculate that the *paracrine* secretion of FGF23 from cardiac fibroblasts together with other factors mediate cardiac hypertrophy and diastolic dysfunction that was observed in mice with transgenic expression of human S100/calgranulin (Figure 7). A possible role for *cardiac-derived* FGF23 in mediating cardiac hypertrophy was previously suggested by a study demonstrating that injection of recombinant FGF23 directly into the myocardium (without detection of rFGF23 in the blood circulation) caused LVH, which was abolished by the pan-FGF receptor inhibitor PD173074 [25]. However, endogenous production of FGF23 within cardiac cells has not been reported to our knowledge. In our animal model, serum FGF23 was equally elevated in hBAC-S100 and WT mice with CKD, while cardiac FGF23 was increased only in the hearts of hBAC-S100 mice. The mechanism whereby FGF23 gene transcription and protein secretion is augmented in the hearts of hBAC-S100 mice with CKD likely represents a response to inflammation since several cytokines were capable to induce FGF23 in cardiac fibroblasts or aortic smooth muscle cells. FGF23 is mainly produced by osteoblasts and chondroblasts in mineralized tissues [28], and recent studies indicated that alterations in matrix mineralization stimulates FGF23 in osteoblasts [34]. However, FGF 23 regulation in VSMC and fibroblast is largely unknown. Our data show that direct treatment of cardiac neonatal fibroblasts with S100A12 protein alone, or together with high phosphate medium, failed to up regulate FGF23 in vitro, indicating other systemic processes mediated by S100/calgranulin. To our knowledge this is the first study to report enhanced FGF23 secretion in cultured vascular cells in response to cytokines. Our hypothesis that FGF23 is induced in response to inflammatory signals in vivo is supported by a recent study by Poess et al. demonstrating a 100-fold increase in serum FGF23 in patients with cardiogenic shock[35]. Although cytokines were not reported in this study, we speculate that the cytokine storm commonly associated with cardiogenic shock may contribute to the severe increase in serum FGF23. We propose that FGF23 could be a link between chronic inflammation and left ventricular hypertrophy, a common cause of diastolic heart failure in patients with diabetes or chronic kidney disease. Our study raises the hypothesis that release of growth factors like FGF23 from activated cardiac fibroblasts in hBAC-S100/CKD hearts could facilitate

pathological cardiac remodeling. Although FGF23 is commonly measured in serum and correlates positively with LVH in patients with chronic kidney disease, future studies are needed to explore cardiac expression of FGF23 and whether this mediates LVH in a paracrine manner. Our *in vitro* data demonstrate cytokine-induced up regulation of FGF23 in cardiac fibroblasts, suggesting that cardiac-derived FGF23 could be a link between systemic inflammation and development of LVH and diastolic heart failure. Supported by recent findings were systemic treatment with pan-FGF receptor inhibitor PD173074 attenuated cardiac hypertrophy in 5/6 nephrectomy rats with CKD[25], future experiments utilizing cardiac specific inhibition of FGF23 are needed to better understand the relationship of FGF23 and cardiac hypertrophy.

A recent epidemiological study in dialysis patients found a positive correlation of serum S100A12 with systemic inflammatory status and with abdominal aortic calcification[3], but to our knowledge it is not known whether serum S100A12 is a biomarker for cardiac calcification or LVH, and whether this would occur independently of serum FGF23. In contrast, serum FGF23 is associated with LVH, but not associated with arterial calcification in patients with CKD, supporting the hypothesis that elevated serum concentrations of FGF23 in patients with CKD primarily affect the heart, but not the arterial vasculature [36].

RAGE was previously shown to mediate diabetic cardiomyopathy [37] and is implicated in cardiac remodeling in response to ischemic injury [383916]. Our study expands these findings and demonstrates that RAGE-mediated systemic inflammation also mediates left ventricular hypertrophy with diastolic dysfunction and accelerated AV thickening and sclerosis in an animal model engineered to mimic human disease, i.e. increased serum S100A12 and uremia. An important role of systemic inflammation is supported by the finding that hBAC-S100/RAGE null hearts lacked FGF23 expression (presumably due to the lack of systemic inflammation) while cultured primary cardiac fibroblasts from RAGE null mice had similar up regulation of FGF23 mRNA and protein levels in response to cytokines. However, future studies are needed to probe whether cardiac myocytes lacking RAGE have a normal hypertrophic response to FGF23 as recently shown for WT cardiac myocytes[25]. Although our data seem to implicate systemic inflammation with increased cytokines as an important mediator of pathological cardiac remodeling in hBAC-S100 mice, we cannot exclude the possibility of increased local inflammation mediated by the infiltration of S100/calgranulin-transgenic myeloid cells. Future work utilizing bone marrow transplant chimeric mice will answer the question whether myeloid-expressed S100/calgranulin is sufficient to give rise to the cartilaginous metaplasia in the hearts of hBAC-S100 mice and whether this depends on bone marrow-derived RAGE or cardiac expressed RAGE. We speculate that the systemic effects in the hBAC-S100 mice with increased serum levels of S100A12, IL-6 and likely other cytokines accounts, at least in part, for the pathological cardiac remodeling. This is supported by our findings that mRNA for S100A12 is absent in primary cardiac fibroblasts and myocytes cultured from hBAC-S100 hearts.

Systemic and local inflammation has been extensively implicated in the progression of calcific aortic valve disease (reviewed in [40]). Our previous work identified enhanced inflammation and oxidative stress in aortic smooth muscle with SM22α-targeted expression of hS100A12 as a sufficient mediator to induce osteoblast- marker genes including DMP1,

Runx2, BMP2, BGLAP and thereby promoting a switch from normal SMCs to calcifying SMCs [19, 41]. Our newly developed mouse model with myeloid-targeted expression of hS100/calgranulin shows enhanced expression of genes regulating inflammation in myeloid cells in a RAGE-dependent manner, and we suggest that RAGE-mediated activation of systemic inflammation could activate cardiac fibroblasts to switch to a chondroblast-like phenotype in vivo. This view is supported by studies where *ENPP1* null mice in combination with loss of RAGE developed less arterial calcification and intra-arterial chondrogenic differentiation compared to *ENPP1* null mice with intact RAGE signaling, indicating an important role for RAGE as modifier of phosphate-mediated calcification [42]. Future research is needed to define detailed mechanisms of how S100/calgranulin promotes osteochondrocytic reprogramming of valvular interstitial fibroblasts. Our data suggests systemic inflammation in vivo, although other mechanisms, for example enhanced susceptibility to attract and harbor circulating osteogenic precursor cells contributing to chondrocytic hyperplasia and annular calcification[40, 43], or the possibility that S100/calgranulin promotes chondroplastic metaplasia of valve cells indirectly by inducing LVH with altered mechanical and hemodynamic forces leading to accelerated valve injury and paracrine signaling from interstitial valve cells [44], can not be excluded. Our finding of reduced osteopontin mRNA in cardiac fibroblasts in response to recombinant S100A12 protein is an unexpected finding, since cytokines, inflammation, and oxidative stress have been shown to increase osteopontin expression in vascular cells [45, 46]. This pleotropic effect of S100A12 on osteopontin regulation needs to be further examined. We speculate that the known pro-inflammatory signaling of S100A12 in combination with a reduction in osteopontin level, an important inhibitor of vascular mineralization, may lead to important insights on the mechanisms of S100A12-mediated calcification of vascular and valvular cell.

The calcification observed in hBAC-S100 mice challenged with CKD was grossly limited to aortic and mitral valve annulus, and we found only scant calcification in the medial layer of the aorta. While at first these findings seem to be in conflict with earlier studies where we reported enhanced medial calcification of the aorta in mice with smooth muscle-targeted expression of human S100A12 using the SM22α promoter and CKD[20], it does suggest that circulating S100/calgranulin protein has a lesser effect on aortic smooth muscle compared to the intracellular expression of S100A12 in smooth muscle either achieved by transgenic engineered cells [19, 20] or in response to injury such as associated with aortic dissection [17].

Taken together, our study provides mechanistic insights into how both biomarkers of increased cardiovascular mortality in CKD, i.e. S100A12 and FGF23, could synergize to provide an environment where S100/RAGE-mediated inflammation promotes up regulation of cardiac-derived FGF23, LVH and diastolic dysfunction together with chondrocytic hypertrophy of the mitral and aortic valve annulus with spotty cardiac calcification. RAGE and its ligands S100/calgranulin are suggested as potential therapeutic targets to attenuate pathological cardiac remodeling in CKD. RAGE was previously shown by our laboratory to initiate pro-inflammatory pathways upon activation by S100A12/EN-RAGE [9]. The presented data implicate for the first time that S100/RAGE is an accelerating factor for the development of cardiac hypertrophy and diastolic dysfunction in a murine model of chronic

kidney disease, and we hypothesize that enhanced FGF23 secretion in cardiac fibrous tissue may promote processes leading to hypertrophy and diastolic dysfunction.

Supplementary Material

Refer to Web version on PubMed Central for supplementary material.

Acknowledgments

The RAGE null mice were a generous gift from Dr. Ann Marie Schmidt, New York University, NY.

Source of funding: This work was supported by the National Health Lung and Blood Institute (1R01HL4821 to MAHB) and an Early Career Award of the Howard Hughes Institute to T.S. Puri.

Non Standard Abbreviations and Acronyms

ANP	atrium natriuretic protein
BUN	blood urea nitrogen
BGLAP	bone gamma-carboxyglutamic acid-containing protein, osteocalcin
CKD	chronic kidney disease
Col1a1	collagen type 1, alpha 1
CTGF	connective tissue growth factor
FGF23, FGF1	Fibroblast growth factor 23, 1
hBAC-S100	human bacterial artificial chromosome containing S100 genes)
LVH	left ventricular hypertrophy
LBP	LPS binding protein
β-MHC	myosin heavy chain β
MGP	matrix Gla protein
OPN	osteopontin
RAGE	receptor for advanced glycation end products
Smad2	mothers against decapentaplegic homolog 2
S100	soluble in 100% ammonium sulfate
TGFβ	Transforming growth factor β
TNFα	Tumor necrosis factor α
VSMC	vascular smooth muscle cells
WT	wild type

References

1. Go AS, Chertow GM, Fan D, McCulloch CE, Hsu CY. Chronic kidney disease and the risks of death, cardiovascular events, and hospitalization. The New England Journal of Medicine. 2004; 351:1296–1305. [PubMed: 15385656]
2. Mori Y, Kosaki A, Kishimoto N, Kimura T, Iida K, Fukui M, Nakajima F, Nagahara M, Urakami M, Iwasaka T, Matsubara H. Increased plasma s100a12 (en-rage) levels in hemodialysis patients with atherosclerosis. Am J Nephrol. 2009; 29:18–24. [PubMed: 18663285]
3. Kim JK, Park S, Lee MJ, Song YR, Han SH, Kim SG, Kang SW, Choi KH, Kim HJ, Yoo TH. Plasma levels of soluble receptor for advanced glycation end products (srage) and proinflammatory ligand for rage (en-rage) are associated with carotid atherosclerosis in patients with peritoneal dialysis. Atherosclerosis. 2012; 220:208–214. [PubMed: 21906738]
4. Shiotsu Y, Mori Y, Hatta T, Maki N, Iida K, Matsuoka E, Kado H, Ishida R, Kishimoto N, Tamagaki K, Nishimura M, Iwamoto N, Ono T, Matsubara H, Kosaki A. Plasma s100a12 levels and peripheral arterial disease in end-stage renal disease. Nephron extra. 2011; 1:242–250. [PubMed: 22470398]
5. Nakashima A, Carrero JJ, Qureshi AR, Miyamoto T, Anderstam B, Barany P, Heimburger O, Stenvinkel P, Lindholm B. Effect of circulating soluble receptor for advanced glycation end products (srage) and the proinflammatory rage ligand (en-rage, s100a12) on mortality in hemodialysis patients. Clin J Am Soc Nephrol. 2010; 12:2213–2219. [PubMed: 20847094]
6. Shiotsu Y, Mori Y, Nishimura M, Sakoda C, Tokoro T, Hatta T, Maki N, Iida K, Iwamoto N, Ono T, Matsuoka E, Kishimoto N, Tamagaki K, Matsubara H, Kosaki A. Plasma s100a12 level is associated with cardiovascular disease in hemodialysis patients. Clin J Am Soc Nephrol. 2011; 6:718–723. [PubMed: 21258041]
7. Shiotsu Y, Mori Y, Nishimura M, Hatta T, Imada N, Maki N, Iida K, Iwamoto N, Matsuoka E, Tamagaki K, Kosaki A. Prognostic utility of plasma s100a12 levels to establish a novel scoring system for predicting mortality in maintenance hemodialysis patients: A two-year prospective observational study in japan. BMC Nephrology. 2013; 14:16. [PubMed: 23324110]
8. Hara M, Ando M, Morito T, Nokiba H, Iwasa Y, Tsuchiya K, Nitta K. S100a12 gene expression is increased in peripheral leukocytes in chronic kidney disease stage 4–5 patients with cardiovascular disease. Nephron Clinical Practice. 2013; 123:202–208. [PubMed: 23921255]
9. Hofmann MA, Drury S, Fu C, et al. Rage mediates a novel proinflammatory axis: A central cell surface receptor for s100/calgranulin polypeptides. Cell. 1999; 97:889–901. [PubMed: 10399917]
10. Yan SF, Ramasamy R, Schmidt AM. The rage axis: A fundamental mechanism signaling danger to the vulnerable vasculature. Circulation Research. 2010; 106:842–853. [PubMed: 20299674]
11. Yan L, Bjork P, Butuc R, Gawdzik J, Earley J, Kim G, Hofmann Bowman MA. Beneficial effects of quinoline-3-carboxamide (abr-215757) on atherosclerotic plaque morphology in s100a12 transgenic apoe null mice. Atherosclerosis. 2013; 228:69–79. [PubMed: 23497784]
12. Edgeworth J, Gorman M, Bennett R, Freemont P, Hogg N. Identification of p8,14 as a highly abundant heterodimeric calcium binding protein complex of myeloid cells. J Biol Chem. 1991; 266:7706–7713. [PubMed: 2019594]
13. Vogl T, Propper C, Hartmann M, Strey A, Strupat K, van den Bos C, Sorg C, Roth J. S100a12 is expressed exclusively by granulocytes and acts independently from mrp8 and mrp14. J Biol Chem. 1999; 274:25291–25296. [PubMed: 10464253]
14. McCormick MM, Rahimi F, Bobryshev YV, Gaus K, Zreiqat H, Cai H, Lord RS, Geczy CL. S100a8 and s100a9 in human arterial wall. Implications for atherogenesis. J Biol Chem. 2005; 280:41521–41529. [PubMed: 16216873]
15. Burke AP, Kolodgie FD, Zieske A, Fowler DR, Weber DK, Varghese PJ, Farb A, Virmani R. Morphologic findings of coronary atherosclerotic plaques in diabetics: A postmortem study. Arterioscler Thromb Vasc Biol. 2004; 24:1266–1271. [PubMed: 15142859]
16. Volz HC, Laohachewin D, Seidel C, Lasitschka F, Keilbach K, Wienbrandt AR, Andrassy J, Bierhaus A, Kaya Z, Katus HA, Andrassy M. S100a8/a9 aggravates post-ischemic heart failure through activation of rage-dependent nf-kappab signaling. Basic Research in Cardiology. 2012; 107:250. [PubMed: 22318783]

17. Das D, Gawdzik J, Dellefave-Castillo L, McNally EM, Husain A, Raman J, Hofmann Bowman MA. S100a12 expression in thoracic aortic aneurysm is associated with increased risk of dissection and perioperative complications. Journal of the American College of Cardiology. 2012; 60:775–785. [PubMed: 22818064]
18. Sakaguchi T, Yan SF, Yan SD, Belov D, Rong LL, Sousa M, Andrassy M, Marso SP, Duda S, Arnold B, Liliensiek B, Nawroth PP, Stern DM, Schmidt AM, Naka Y. Central role of rage-dependent neointimal expansion in arterial restenosis. J Clin Invest. 2003; 111:959–972. [PubMed: 12671045]
19. Hofmann Bowman MA, Gawdzik J, Bukhari U, Husain AN, Toth PT, Kim G, Earley J, McNally EM. S100a12 in vascular smooth muscle accelerates vascular calcification in apolipoprotein e-null mice by activating an osteogenic gene regulatory program. Arterioscler Thromb Vasc Biol. 2011; 31:337–344. [PubMed: 20966394]
20. Gawdzik J, Mathew L, Kim G, Puri TS, Hofmann Bowman MA. Vascular remodeling and arterial calcification are directly mediated by s100a12 (en-rage) in chronic kidney disease. Am J Nephrol. 2011; 33:250–259. [PubMed: 21372560]
21. Fuellen G, Nacken W, Sorg C, Kerkhoff C. Computational searches for missing orthologs: The case of s100a12 in mice. OMICS. 2004; 8:334–340. [PubMed: 15703480]
22. Hofmann Bowman M, Wilk J, Heydemann A, Kim G, Rehman J, Lodato JA, Raman J, McNally EM. S100a12 mediates aortic wall remodeling and aortic aneurysm. Circulation Research. 2010; 106:145–154. [PubMed: 19875725]
23. Chellan B, Yan L, Sontag TJ, Reardon CA, Hofmann Bowman MA. Il-22 is induced by s100/calgranulin and impairs cholesterol efflux in macrophages by down regulating abcg1. Journal of Lipid Research. 2014; 55:443–454. [PubMed: 24367046]
24. Carlstrom M, Sallstrom J, Skott O, Larsson E, Wahlin N, Persson AEG. Hydronephrosis causes salt-sensitive hypertension and impaired renal concentrating ability in mice. Acta Physiol. 2007; 189:293–301.
25. Faul C, Amaral AP, Oskouei B, Hu MC, Sloan A, Isakova T, Gutierrez OM, Aguillon-Prada R, Lincoln J, Hare JM, Mundel P, Morales A, Scialla J, Fischer M, Soliman EZ, Chen J, Go AS, Rosas SE, Nessel L, Townsend RR, Feldman HI, St John Sutton M, Ojo A, Gadegbeku C, Di Marco GS, Reuter S, Kentrup D, Tiemann K, Brand M, Hill JA, Moe OW, Kuro OM, Kusek JW, Keane MG, Wolf M. Fgf23 induces left ventricular hypertrophy. J Clin Invest. 2011; 121:4393–4408. [PubMed: 21985788]
26. Gutierrez OM, Mannstadt M, Isakova T, Rauh-Hain JA, Tamez H, Shah A, Smith K, Lee H, Thadhani R, Juppner H, Wolf M. Fibroblast growth factor 23 and mortality among patients undergoing hemodialysis. The New England Journal of Medicine. 2008; 359:584–592. [PubMed: 18687639]
27. Park SH, Stenvinkel P, Lindholm B. Cardiovascular biomarkers in chronic kidney disease. Journal of Renal Nutrition. 2012; 22:120–127. [PubMed: 22200428]
28. Yoshiko Y, Wang H, Minamizaki T, Ijuin C, Yamamoto R, Suemune S, Kozai K, Tanne K, Aubin JE, Maeda N. Mineralized tissue cells are a principal source of fgf23. Bone. 2007; 40:1565–1573. [PubMed: 17350357]
29. Shuvy M, Abedat S, Beeri R, Danenberg HD, Planer D, Ben-Dov IZ, Meir K, Sosna J, Lotan C. Uraemic hyperparathyroidism causes a reversible inflammatory process of aortic valve calcification in rats. Cardiovascular Research. 2008; 79:492–499. [PubMed: 18390899]
30. Shuvy M, Abedat S, Beeri R, Valitsky M, Daher S, Kott-Gutkowski M, Gal-Moscovici A, Sosna J, Rajamannan NM, Lotan C. Raloxifene attenuates gas6 and apoptosis in experimental aortic valve disease in renal failure. American Journal of Physiology Heart and Circulatory Physiology. 2011; 300:H1829–1840. [PubMed: 21335463]
31. Harja E, Bu DX, Hudson BI, et al. Vascular and inflammatory stresses mediate atherosclerosis via rage and its ligands in apoe−/− mice. J Clin Invest. 2008; 118:183–194. [PubMed: 18079965]
32. Isakova T, Xie H, Yang W, Xie D, Anderson AH, Scialla J, Wahl P, Gutierrez OM, Steigerwalt S, He J, Schwartz S, Lo J, Ojo A, Sondheimer J, Hsu CY, Lash J, Leonard M, Kusek JW, Feldman HI, Wolf M. Chronic Renal Insufficiency Cohort Study G. Fibroblast growth factor 23 and risks of mortality and end-stage renal disease in patients with chronic kidney disease. JAMA. 2011; 305:2432–2439. [PubMed: 21673295]

33. Gutierrez OM, Januzzi JL, Isakova T, Laliberte K, Smith K, Collerone G, Sarwar A, Hoffmann U, Coglianese E, Christenson R, Wang TJ, deFilippi C, Wolf M. Fibroblast growth factor 23 and left ventricular hypertrophy in chronic kidney disease. Circulation. 2009; 119:2545–2552. [PubMed: 19414634]
34. Martin A, Liu S, David V, Li H, Karydis A, Feng JQ, Quarles LD. Bone proteins phex and dmp1 regulate fibroblastic growth factor fgf23 expression in osteocytes through a common pathway involving fgf receptor (fgfr) signaling. FASEB. 2011; 25:2551–2562.
35. Poss J, Mahfoud F, Seiler S, Heine GH, Fliser D, Bohm M, Link A. Fgf-23 is associated with increased disease severity and early mortality in cardiogenic shock. European Heart Journal. Acute Cardiovascular Care. 2013; 2:211–218. [PubMed: 24222832]
36. Scialla JJ, Lau WL, Reilly MP, et al. Fibroblast growth factor 23 is not associated with and does not induce arterial calcification. Kidney International. 2013; 83:1159–1168. [PubMed: 23389416]
37. Nielsen JM, Kristiansen SB, Norregaard R, Andersen CL, Denner L, Nielsen TT, Flyvbjerg A, Botker HE. Blockage of receptor for advanced glycation end products prevents development of cardiac dysfunction in db/db type 2 diabetic mice. European Journal of Heart Failure. 2009; 11:638–647. [PubMed: 19502378]
38. Bucciarelli LG, Ananthakrishnan R, Hwang YC, Kaneko M, Song F, Sell DR, Strauch C, Monnier VM, Yan SF, Schmidt AM, Ramasamy R. Rage and modulation of ischemic injury in the diabetic myocardium. Diabetes. 2008; 57:1941–1951. [PubMed: 18420491]
39. Tsoporis JN, Izhar S, Leong-Poi H, Desjardins JF, Huttunen HJ, Parker TG. S100b interaction with the receptor for advanced glycation end products (rage): A novel receptor-mediated mechanism for myocyte apoptosis postinfarction. Circulation Research. 2010; 106:93–101. [PubMed: 19910580]
40. Rajamannan NM, Evans FJ, Aikawa E, Grande-Allen KJ, Demer LL, Heistad DD, Simmons CA, Masters KS, Mathieu P, O'Brien KD, Schoen FJ, Towler DA, Yoganathan AP, Otto CM. Calcific aortic valve disease: Not simply a degenerative process: A review and agenda for research from the national heart and lung and blood institute aortic stenosis working group. Executive summary: Calcific aortic valve disease-2011 update. Circulation. 2011; 124:1783–1791. [PubMed: 22007101]
41. Towler DA. Vascular calcification: It's all the rage! Arterioscler Thromb Vasc Biol. 2011; 31:237–239. [PubMed: 21248279]
42. Cecil DL, Terkeltaub RA. Arterial calcification is driven by rage in enpp1−/− mice. Journal of Vascular Research. 2011; 48:227–235. [PubMed: 21099228]
43. Rajamannan NM. Calcific aortic valve disease: Cellular origins of valve calcification. Arterioscler Thromb Vasc Biol. 2011; 31:2777–2778. [PubMed: 22096095]
44. Li C, Xu S, Gotlieb AI. The progression of calcific aortic valve disease through injury, cell dysfunction, and disruptive biologic and physical force feedback loops. Cardiovascular Pathology. 2013; 22:1–8. [PubMed: 22795219]
45. Lyle AN, Remus EW, Fan AE, Lassegue B, Walter GA, Kiyosue A, Griendling KK, Taylor WR. Hydrogen peroxide regulates osteopontin expression through activation of transcriptional and translational pathways. J Biol Chem. 2014; 289:275–285. [PubMed: 24247243]
46. Giachelli CM, Speer MY, Li X, Rajachar RM, Yang H. Regulation of vascular calcification: Roles of phosphate and osteopontin. Circulation Research. 2005; 96:717–722. [PubMed: 15831823]

Significance

Left ventricular hypertrophy, diastolic dysfunction and ectopic valvular calcification are common cardiovascular complication in patients with chronic kidney disease. Our study utilizes a newly generated mouse model with transgenic expression of human S100/calgranulins targeted to myeloid cells. We could demonstrate that myeloid-derived hS100/calgranulin is sufficient to induce systemic inflammation and this is associated with accelerated LVH and valve disease in mice challenged with chronic kidney disease. This is abolished in mice lacking RAGE, the Receptor for Advanced Glycation Endproducts. We speculate that the enhanced systemic inflammation present in hBAC-S100 mice leads to the observed increased expression of FGF23 in the cardiac tissue, since cytokines (TNFα, IL-6, LPS) directly induce FGF23 in cultured primary cardiac fibroblasts. We hypothesize that the inflammation-mediated expression of FGF23 in cardiac fibroblasts may act in a paracrine manner to induce LVH, thereby providing a possible link between inflammation and LVH with diastolic dysfunction.

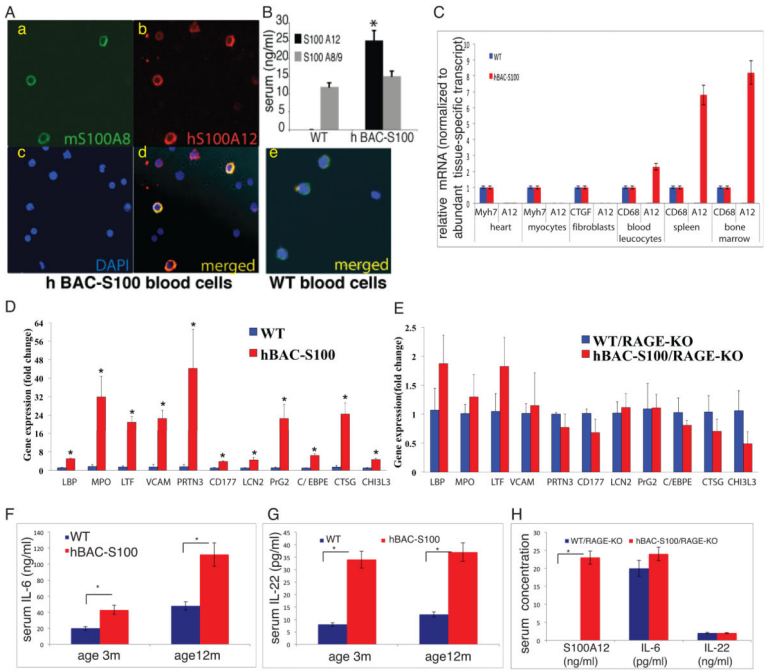

Figure 1. Transgenic expression of human S100/calgranulin in myeloid cells is associated with inflammation

A) Transgenic expression of a bacterial artificial chromosome containing the human S100/calgranulin genes (hBAC-S100) up regulates protein expression of S100A12 in myeloid blood cells (red-stained cells on immunofluorescent microscopy insert b) and not in WT peripheral blood cells (insert e). **B)** S100A12 is increased in serum of hBAC-S100 mice and not detectable in WT serum (* $p<0.001$). **C)** qRT-PCR for S100A12mRNA normalized to β-actin and expressed as fold change compared to the expression of a tissue-specific abundant gene (myosin heavy chain 7, Myh7 for heart tissue and isolated cardiac myocytes; connective tissue growth factor, CTGF for isolated cardiac fibroblasts; CD68 for peripheral blood leucocytes, spleen, and bone marrow). **D/E)** qRT-PCR from peripheral blood cDNA of 6-week-old WT and hBAC-S100 littermate mice with intact RAGE signaling (D) and from 6-week-old WT and hBAC-S100 littermate mice with deleted RAGE signaling (RAGE-KO) (E) for LPS-binding protein (LBP), myeloperoxidase (MPO), neutrophil lactoferrin (LTF), vascular cell adhesion molecule 1 (VCAM1), neutrophil proteinase 4 (PRTN3), human neutrophil alloantigen 2a (CD177), neutrophil gelatinase-associated lipocalin (LCN2), proteoglycan 2, bone marrow (PRG2), CCAAT/enhancer binding protein (C/EBP), epsilon (CEBPE), cathepsin G (CTSG), and chitinase 3-like 3 (CHI3l3). **F/G)** Serum IL-6 and IL-22 are increased in hBAC-S100 mice with intact RAGE, **H)** attenuated IL-6 and IL-22 in mice lacking RAGE (WT and hBAC-S100) despite expression of S100A12 in hBAC/S100-RAGE KO mice (*$P<0.03$).

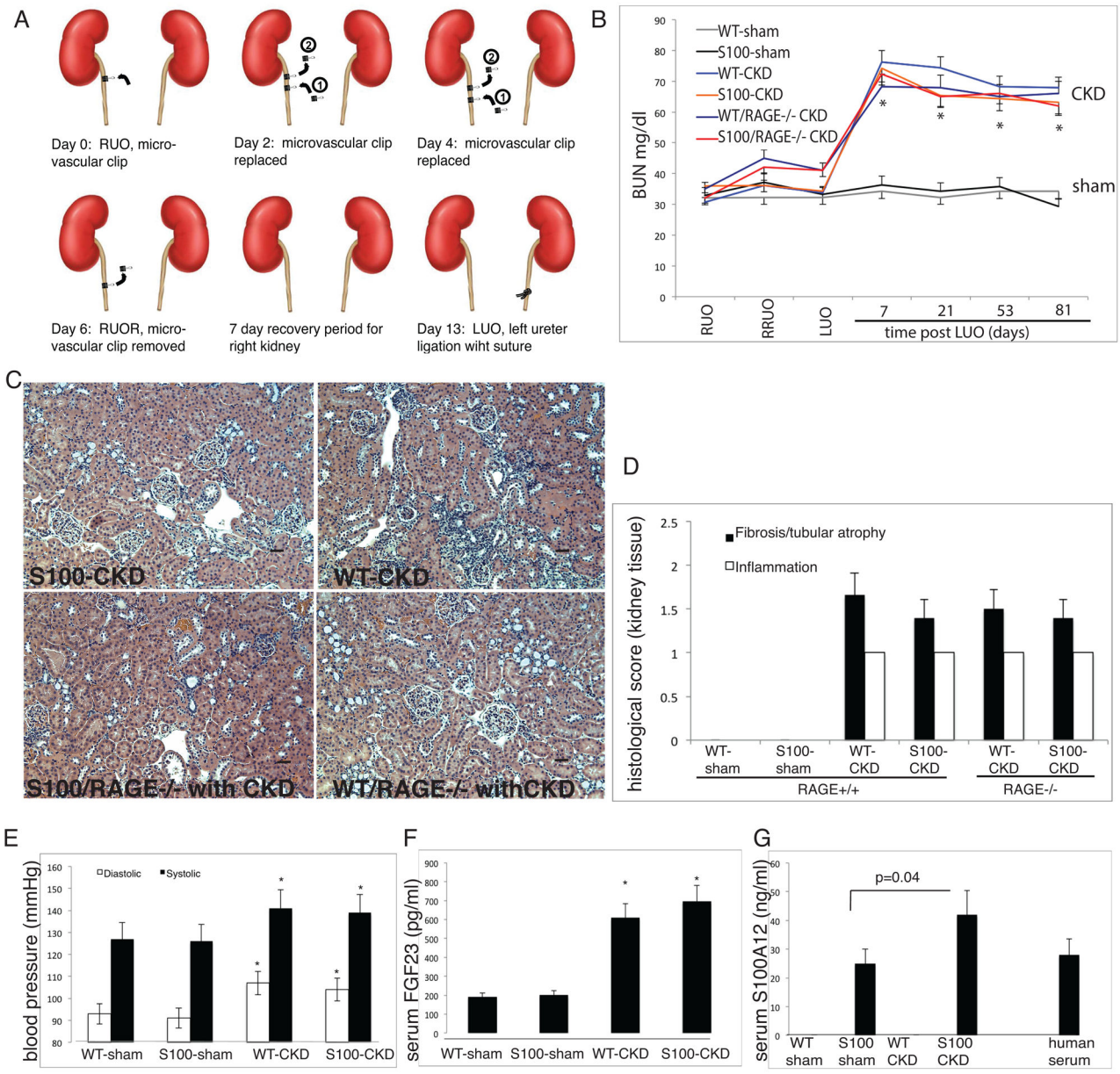

Figure 2. Model of CKD in hBAC-S100 and WT littermate mice

A) Reversible surgical ligation of the right ureter followed by irreversible ligation of the left ureter. **B)** BUN was measured in the serum at various time points until sacrifice as an indicator for developing CKD after reversible right ureter obstruction (RUO) for 6 days, followed by release of RUO (RRUO), followed 7 days later by irreversible left ureter obstruction (LUO). * P=0.001 vs. sham). **C/D)** Representative H&E stained slides of the right kidney were scored for interstitial fibrosis with tubular atrophy, and for interstitial inflammation using scores of 0–3 for semi-quantitative assessment with 0 =<5%, 1= 6–25%, 2= 26–50%, and 3=>50% involvement. There was no difference in renal pathology between the four CKD groups. Scale bar 10 μm. **E)** Systolic and diastolic blood pressure were measured in the tail artery (* P=0.04 vs. respective sham group). **F)** Serum FGF23 and

S100A12 **(G)** were measured by ELISA (* P=0.01 vs. respective sham group). All values are mean ±SEM, n>20 mice per group.

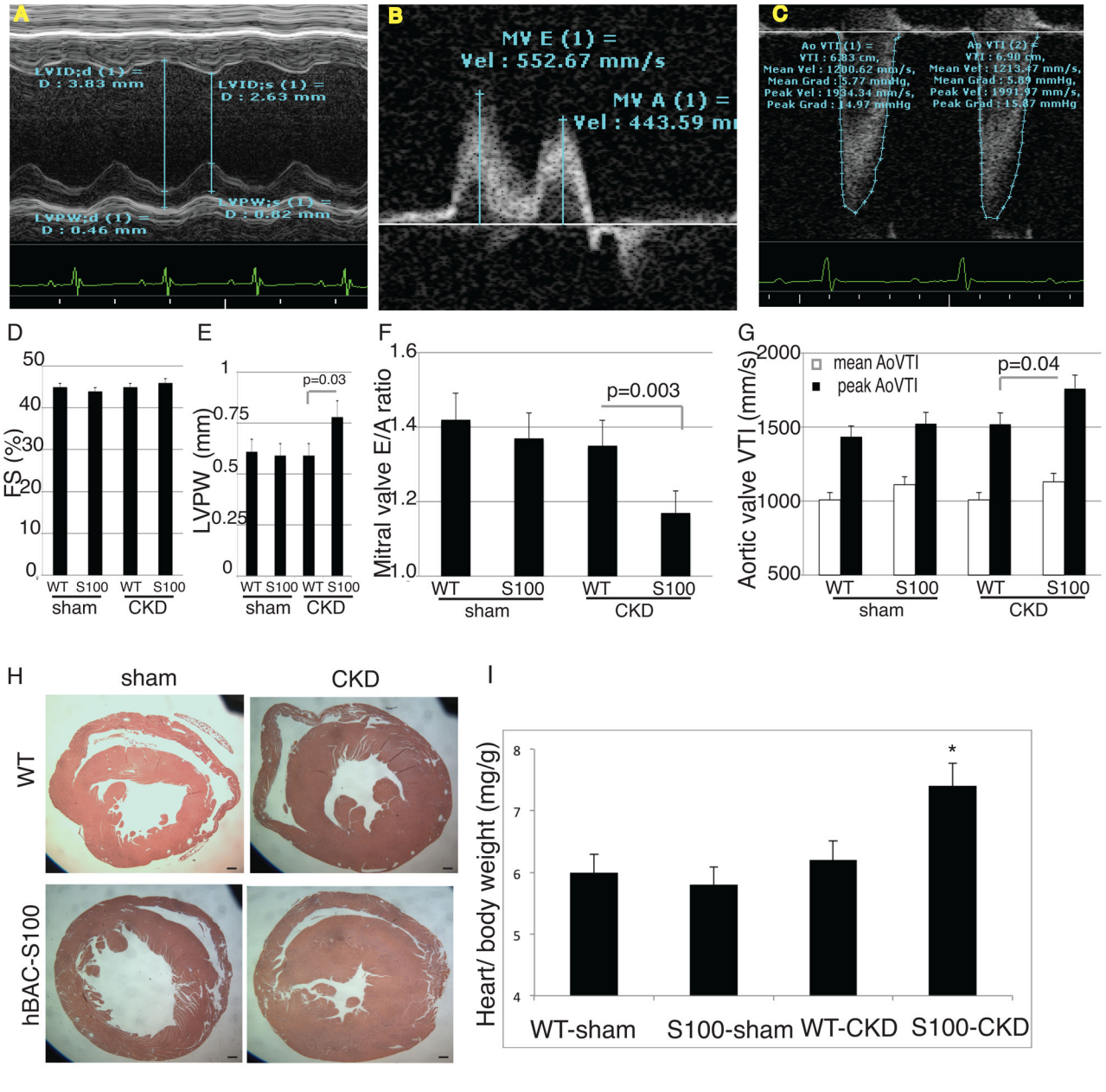

Figure 3. hBAC-S100 mice with CKD develop LVH and impaired diastolic function

A) M-mode Doppler for measurement of fractional shortening (FS, quantified in D) and Left Ventricular Posterior Wall Thickness (LVPW, quantified in E). **B)** Continuous wave Doppler over the mitral valve for early (E) and atrial (A) flow was measured to calculate E/A (quantified in F). **C)** Continuous wave Doppler over the aortic valve was measured to calculate mean and peak aortic valve velocity timed integral (AoVTI, quantified in G). **H)** Representative gross pathology sections from the cardiac mid-chamber (hematoxylin and eosin stain, 5x magnification, scale bare = 20 μm) demonstrate LVH, confirmed by **(I)** increased ratio of heart weight to body weight in hBAC-S100/CKD mice (* P= 0.01 compared to WT/CKD and S100/sham). All values are mean ±SEM, n>20 mice per group.

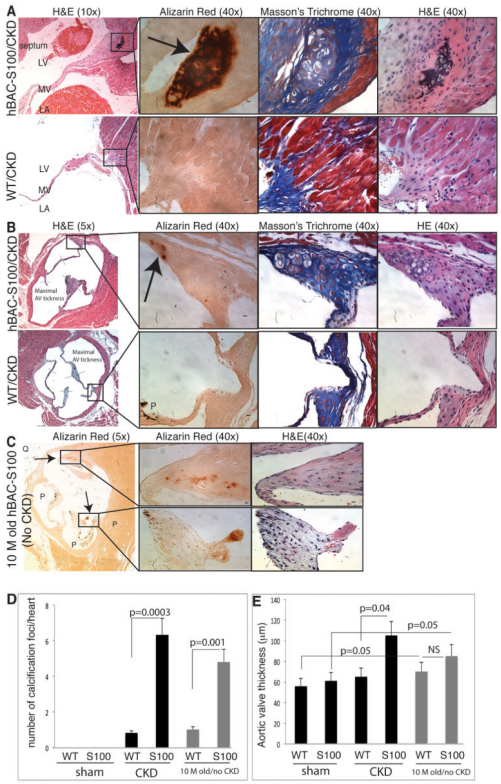

Figure 4. hBAC-S100 mice with CKD develop ectopic cardiac calcification

A) Serial stained sections of the mitral valve of hBAC-S100 (upper panel) and WT mice (lower panel) and **B)** of the aortic valve of hBAC-S100 (upper panel) and WT mice (lower panel). Serial sections were stained for hematoxylin and eosin (H&E), Alizarin Red S staining calcium deposits in red color as marked by arrow, and Masson's Trichrome. P=pigment, Scale bar 10 μm. **C)** Cardiac calcification developed spontaneously in 10-month-old hBAC-S100 mice (without CKD and on regular rodent chow diet) as shown by red color on Alizarin Red S stained sections of the aortic valve and co-localizing to hypertrophic chondroblast-like cells (upper panel in C), and to calcification on the valve leaflet tip (lower panel in C). **D)** Red-colored calcification foci (shown by arrow) but not the black-colored pigment deposition (marked as P) on Alizarin Red S-stained serial sections (n= 50–70 per heart) were counted from the apex to the ascending aorta. **E)** Quantification of the maximal aortic valve thickness of the three leaflets measured as depicted in panel B. All values are mean ±SEM, n=10 mice per group.

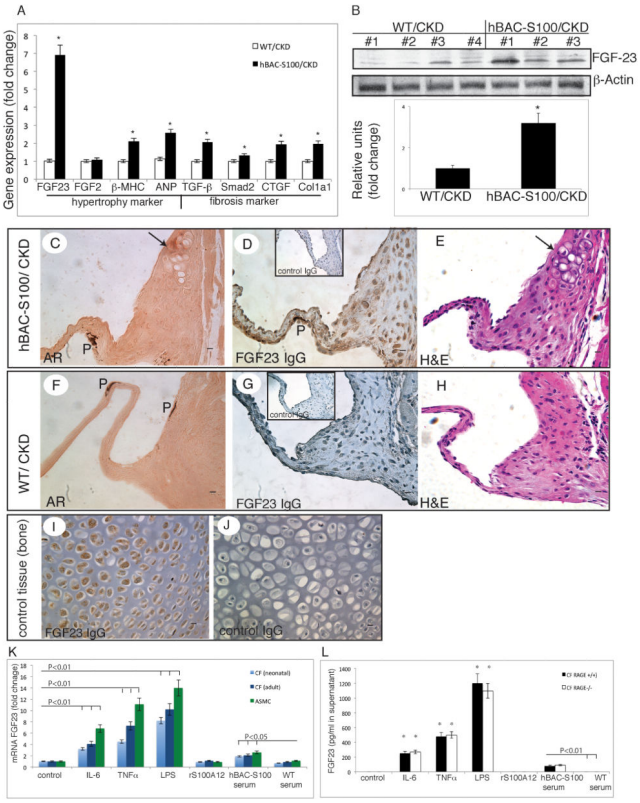

Figure 5. hBAC-S100 mice with CKD develop left ventricular hypertrophy

A) Quantitative real time RT-PCR in murine heart for genes associated with hypertrophy and fibrosis. **B)** Immunoblotting of cardiac tissue lysates for FGF23 and β actin, and semiquantitave densitometry of bands. **C–J)** Serial sections of the aortic valve of hBAC-S100 (C–E) and WT control (F–H) stained with Alizarin Red (C, F) and hematoxylin and eosin (E, H) shows calcifying chondroblast-like cells (marked with an arrow) and expression of FGF23 in interstitial valve cells in hBAC-S100 mice (D) but not in WT mice (G). Non-immune IgG was used as negative control (insert in D & G, J), and newborn murine WT bone tissue was used as positive control (I). 400x magnification, scale bare = 10 μm, P=pigment. **K.** Quantitative real time RT-PCR in cultured primary murine cardiac fibroblasts (CF) and aortic smooth muscle cells (ASMC) for FGF23 mRNA after 6h stimulation with IL-6 (25 ng/ml), TNFα (25 ng/ml) LPS (25 ng/ml), recombinant S100A12 (2 ug/ml), serum from hBAC-S100 mice (3%) or serum from WT mice (3%). **L.** FGF23 protein measured by ELISA in cell culture supernatant from primary neonatal cardiac fibroblast from WT/RAGE+/+ and WT/RAGE−/− mice after 24 hours stimulated with cytokines or mouse serum (* P<0.01 compared to control)

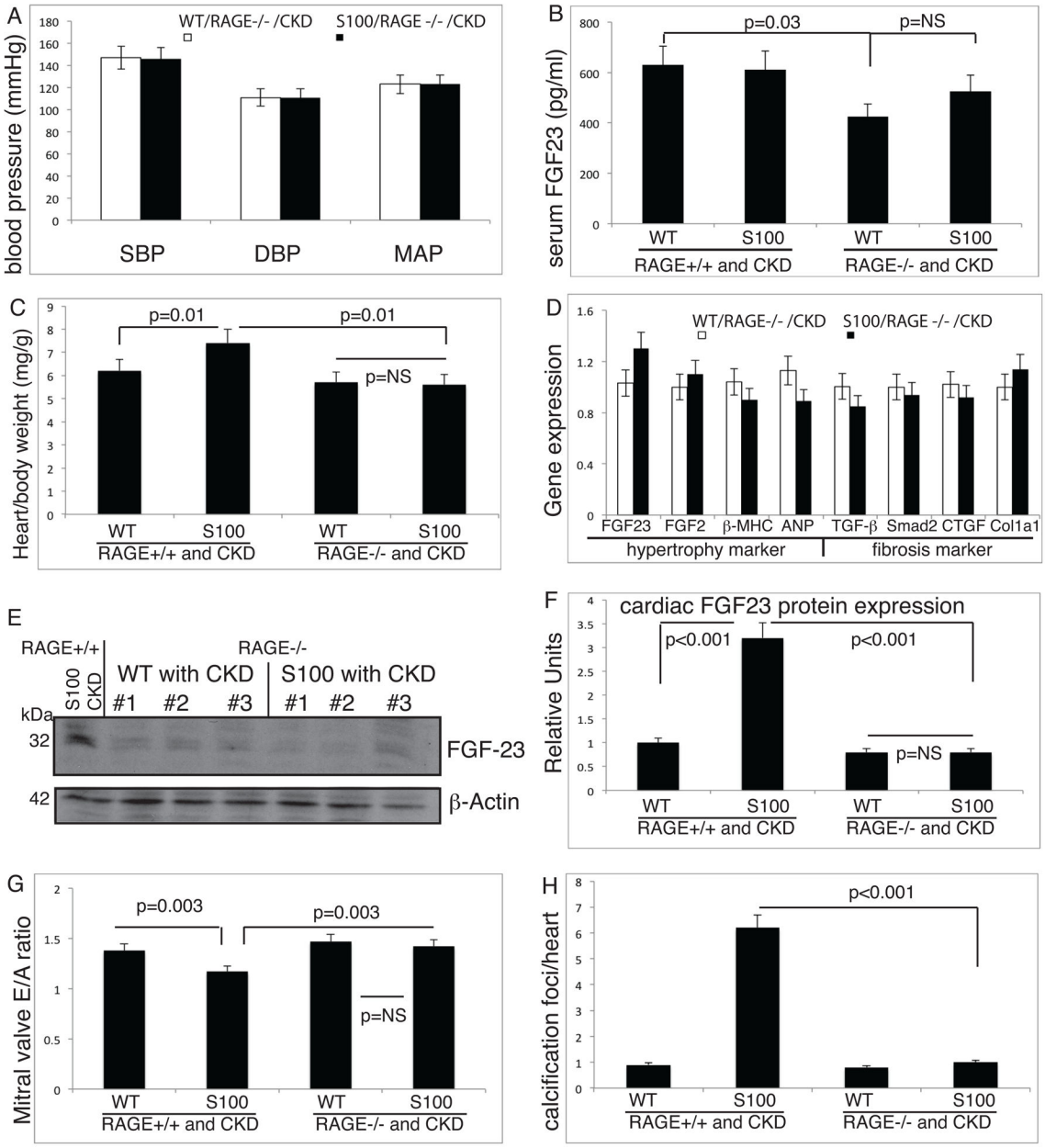

Figure 6. hBAC-S100 mice with CKD and lacking RAGE are protected from cardiac hypertrophy and calcification

A) Systolic (SBP), diastolic (DBP) and mean (MAP) arterial blood pressure were measured in the tail artery. **B)** Serum FGF23 was measured by ELISA. **C)** Indexed heart weight to body weight measured at sacrifice. **D)** Quantitative real time RT-PCR in murine hearts for selected genes associated with hypertrophy and fibrosis. **E)** Immunoblotting of cardiac tissue lysates for FGF23 and β actin, including hBAC-S100/RAGE+/+/CKD as positive control (left lane), and from mice lacking RAGE (lane 2–7), and semiquantitative densitometry of bands **(F). G)** E/A ratio of continuous wave Doppler over the mitral valve for early (E) and atrial (A) flow is calculated as a measure of diastolic function. **H)**

Quantification of red-colored calcification foci on Alizarin Red S-stained serial cardiac sections 200 μm apart was counted from the apex to the ascending aorta.

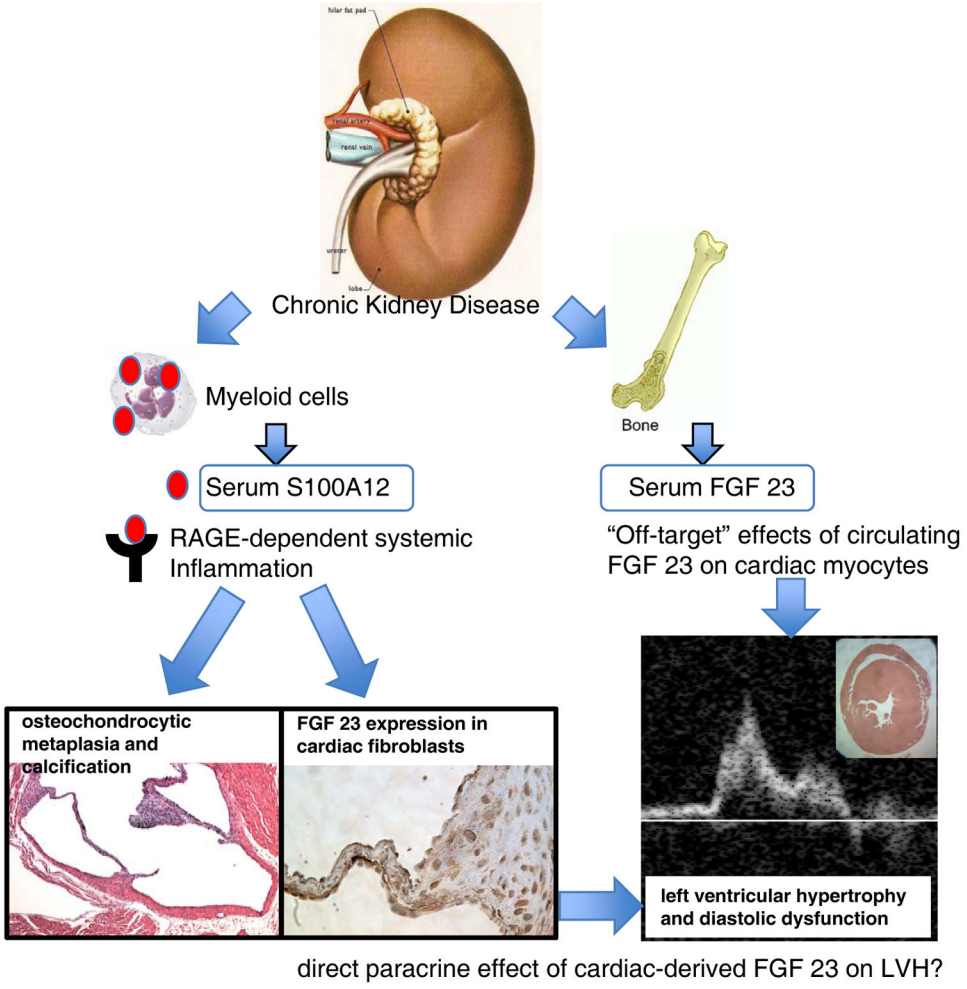

Figure 7. Proposed model of LVH in CKD

Increased serum concentration of S100/calgranulins in mice with CKD promotes systemic inflammation in a RAGE-dependent manner, and this is associated with cartilagenous metaplasia and calcification of the valve annulus. Importantly, systemic inflammation in vivo (and in cultured cardiac fibroblasts upon treatment with cytokines), up regulates endogenous FGF23 in cardiac fibroblasts, which may act in a paracrine manner to promote LVH and diastolic dysfunction. Elevated serum FGF23 has been previously associated with LVH and recombinant FGF23 was shown to directly cause hypertrophy of cardiac myocytes in vitro and in vivo (ref. 24).